

## Article

# Fabrication, Design and Characterization of 1D Nano-Fibrous SiO<sub>2</sub> Surface by a Facile and Scalable Method

Lahcen Khouchaf <sup>1,\*</sup> and Abdelhamid Oufakir <sup>2</sup>

<sup>1</sup> IMT Nord Europe, Lille University, Cité Scientifique, Rue Guglielmo Marconi, CEDEX, 59653 Villeneuve D'Ascq, France

<sup>2</sup> Department of Chemistry, Faculty of Science, Cadi Ayyad University, Marrakech 40000, Morocco; oufakir.emi@gmail.com

\* Correspondence: lahcen.khouchaf@imt-nord-europe.fr

**Abstract:** In this paper, new 1D nano-fibrous SiO<sub>2</sub> with functionalized surfaces is prepared. First, the effect of dispersion on the morphology and the surface properties of the silica SiO<sub>2</sub> compounds are investigated. Second, energy dispersive spectrometer (EDS) and variable pressure scanning electron microscope (VP-SEM) show typically pure and fibrous texture on the surface of SiO<sub>2</sub>. Third, the presence of the bridging oxygen stretching vibration Si-O-Si, as well as the increase in the intensity ratio between Si-OH band and Si-O-Si are revealed by (FTIR) spectroscopy. Furthermore, X-ray diffraction (XRD) validates the conservation of the SiO lattice after chemical treatment through the KOH for both dispersed and non-dispersed samples. In addition, the shift of the XRD main peak (101) is in good agreement with the FTIR results showing the shift of Si-O-Si peak and the increase in the intensity ratio of Si-OH/Si-O-Si. The dispersed SiO<sub>2</sub> sample exhibits a promising functionalized surface with satisfactory results in terms of silica nanofibers crystallinity and chemical composition. As a result, high resolution transmission electron microscopy (HR-TEM) data corroborate the claim of the presence of SiO<sub>2</sub> nanofibers on the surface from 20 nm to 250 nm. New nano-fibrous SiO<sub>2</sub> surfaces will be used to improve interfacial bonding strength between SiO<sub>2</sub> compounds and polymer (or organic materials).

**Keywords:** functionalized surface; dispersion; 1D SiO<sub>2</sub> nano-fibers; silanols; HR-TEM



**Citation:** Khouchaf, L.; Oufakir, A. Fabrication, Design and Characterization of 1D Nano-Fibrous SiO<sub>2</sub> Surface by a Facile and Scalable Method. *Crystals* **2022**, *12*, 531. <https://doi.org/10.3390/cryst12040531>

## Academic Editors:

Jesús Sanmartín-Matalobos and Karl S. Coleman

Received: 26 February 2022

Accepted: 8 April 2022

Published: 10 April 2022

**Publisher's Note:** MDPI stays neutral with regard to jurisdictional claims in published maps and institutional affiliations.



**Copyright:** © 2022 by the authors. Licensee MDPI, Basel, Switzerland. This article is an open access article distributed under the terms and conditions of the Creative Commons Attribution (CC BY) license (<https://creativecommons.org/licenses/by/4.0/>).

## 1. Introduction

There is a large number of natural and synthetic SiO<sub>2</sub> compounds with high mechanical and thermal properties that are eco-friendly materials promoting ecology and sustainable development, and can be outstanding candidates for replacing some synthetic fibers in the automobile and packaging industries, as an example [1,2]. In addition, SiO<sub>2</sub> compounds have found interesting applications in a variety of disciplines, including materials science [3,4], catalysis and clean technology [5,6], separations science, and microelectronics devices [7]. Silica is also a good candidate as a filler in composite polymers [8–10]. However, the use of SiO<sub>2</sub> compounds usually suffers from some disadvantages, such as poor interfacial bonding strength between SiO<sub>2</sub> compounds and polymer matrix (or organic materials), and surface flaws on natural fibers degrading its tensile properties [11,12]. These disadvantages would affect the mechanical and thermal properties of composites based on SiO<sub>2</sub> as a filler [13]. Thus, in order to overcome these inconveniences, new SiO<sub>2</sub> surfaces must be developed.

In fact, various possibilities exist to modify the surface of reinforcing polymers by fibers in order to enhance the cohesive interactions at the interface. Some cohesive interactions between polymer and fibers may involve co-crystallization phenomena and the development of robust structures with a gradient structure at the interface. Thus, the properties are gradually changing from the interface toward the bulk matrix involving a change in mechanical properties and the rheology of certain asphalts for example.

The reactive ability of silica mainly comes from the presence of silanol Si-OH groups on their surface [14–17]. Furthermore, the surface of SiO<sub>2</sub> compounds, enriched with Si-O-Si siloxane groups is much less reactive than with silanol ones. Therefore, to increase the reactive ability of the silica surfaces and to be able to interact with the molecules of modifiers, it is necessary to create more silanol groups on their surface. All reactions of the further modification take place with the implementation of silanol groups. One way to increase the concentration of silanol groups on the surface of silica is to submit SiO<sub>2</sub> compounds to KOH solution, which leads to break down the Si-O-Si network with the creation of silanols groups Si-OH.

In fact, a good dispersion of SiO<sub>2</sub> particles is an important parameter, offering a big surface exchange. According to the literature, the PZC (point zero charge) of silica SiO<sub>2</sub> is located between pH 2 and pH 3 [18–20]. The surface of silica is positively charged SiO<sub>2</sub><sup>+</sup>: silica becomes possible anions exchange (SiOH<sub>2</sub><sup>+</sup> ↔ SiOH + H<sup>+</sup>) below the PZC and negatively charged above the PZC SiO<sub>2</sub><sup>-</sup>: silica becomes possible cations exchange [21–23].



In this research paper, new fibrous SiO<sub>2</sub> surfaces are prepared. The effect of dispersion on the morphology and the surface properties of the silica SiO<sub>2</sub> compounds are investigated. The characterization of surface modification and morphology was investigated using VP-SEM, HR-TEM, EDS, FTIR, XRD, and XPS.

## 2. Materials and Methods

### 2.1. Samples Preparation

The material used in this work is a natural 99.9% SiO<sub>2</sub> flint from the north of France called “SilB”. The samples were prepared using the procedure given in Figure 1. A solution of hydrochloric acid HCl (V = 10 ML, pH = 3.5) is prepared and 1 g of the starting SiO<sub>2</sub> sample (SilB) is introduced. The mixture is stirred for 1 h, and then the suspension is allowed to stand for 24 h. After the dispersion step, the dispersed sample was recovered from the solution by filtration. In fact, the reaction with KOH solution was carried out as follows: The siliceous natural aggregate sample was put in the autoclave in an oven at 80 °C. After 30 min of preheating, we have added a 10 ML of KOH solution with a concentration of 0.79 mol/L.

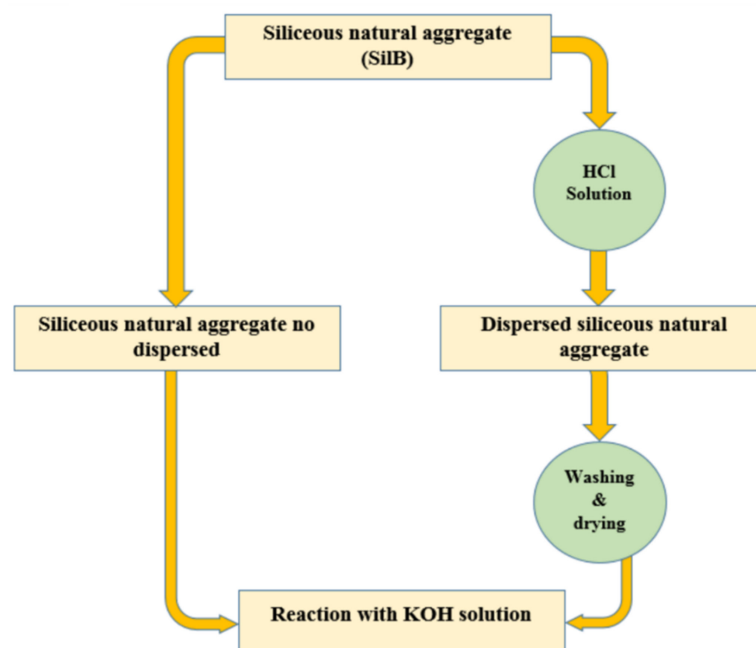


Figure 1. Preparation protocol diagram.

The mixture was then put in an oven to develop a reaction under controlled temperature and reaction time. After the reaction time, we introduced the autoclave in frozen water for 5 min to stop the reaction. Afterward, the soluble reaction products were removed by selective acid treatment and filtration. The acid treatment is done using 250 mL cold HCl solution (0.5 M). The samples were dried by acetone and diethyl ether treatment after the filtration and then kept inside a dried atmosphere. In the rest of the text, the starting SiO<sub>2</sub> sample, the reacted SiO<sub>2</sub> sample without dispersion, and the reacted SiO<sub>2</sub> sample with dispersion in HCl solution with pH = 3.5 are named (SilB), (Siland), (Silad3.5) respectively.

## 2.2. Characterization

Compounds have been characterized by variable pressure scanning electron microscopy (VP-SEM), X-ray diffraction (XRD), Fourier-transformed infrared spectroscopy (FTIR), and HR-transmission electron microscopy (HR-TEM). Energy dispersive spectrometry was used to check the purity of the samples after chemical treatment.

### 2.2.1. HR-TEM and VP-SEM

The morphology of surface silica samples was characterized with variable pressure scanning electron microscopy (VP-SEM) using VEGA 3 instrument model, product by TESCAN and using an accelerating voltage of 10 kV. It is coupled to the energy dispersive X-ray spectroscopy (EDS). In addition, high resolution transmission electron microscopy (HR-TEM) a Titan Themis STEM microscopy (80 kV) equipped with an EDS detector to visualize the morphology of the surface silica were used to image the nanostructures of the samples. Using a low accelerating voltage keeps the sample free from electron beam artifacts.

### 2.2.2. Fourier Transformed Infrared Spectroscopy (FTIR)

FTIR spectra of silica samples were acquired with a Bruker VERTEX 70 spectrometer in reflection mode. They were recorded by collecting 100 scans at 4 cm<sup>-1</sup> resolution in the range of 400–4000 cm<sup>-1</sup>.

### 2.2.3. X-ray Photoelectron Spectroscopy XPS

The XPS measurements were performed using a spectrometer with a monochromatized AlK $\alpha$  X-ray source ( $h\nu = 1486.6$  eV). The data were collected on the dried and powdered samples which are pressed onto a substrate and is fixed on a sample holder. The samples are introduced successively in a chamber at a constant pressure ( $P = 10^{-3}$  torr) and in an analytical chamber ( $P = 10^{-9}$  torr). The ejected electrons photoelectrons whose binding energies are inferior to the X-ray energy are collected according to their kinetic energies into a hemispherical 150 mm mean radius electron analyzer.

### 2.2.4. X-ray Diffraction

XRD measurements were performed in the reflection mode using a Bruker D8 Advance diffractometer (Cu-K  $\lambda$  radiation = 1.5406 Å), operating at 40 kV and 40 mA. Data were recorded in the range of 5°–70° in the 2 $\theta$  scale with a step size of 0.02° and a counting time of 0.5 s/step. Diffraction pattern of each sample was obtained by plotting intensity of diffraction versus double Bragg angle. Data treatment was done using «HighScore» software.

## 3. Results

### 3.1. Variable Pressure Scanning Electron Microscopy (VP-SEM)

Figure 2 shows VP-SEM images of the SiO<sub>2</sub> sample surface-treated under different conditions. Before reaction, the grains have a well-defined shape with a relatively smooth surface (Figure 2a).

Moreover, the grains have different sizes ranging from a hundred nanometers to a few micrometers. In addition, the angular sides and the angles of the grains, characteristic of

quartz are clearly seen. After reaction without dispersion, a morphology change with less well-defined forms is observed, compared to the untreated sample (Figure 2b).

Contrariwise, a significant change in the morphology of the grains occurs after dispersion (Figure 2c) with the formation of grains having a fibrous surface. The origin of the different grains forms is due to the breaking up of siloxane bonds by hydroxide ions and the formation of silanols groups as confirmed below, which are the key parameter when  $\text{SiO}_2$  is used for applications involving the functionalization of the material. This result is interesting for future studies since it leads to the improvement of the interface properties of some composites materials with the presence of  $\text{SiO}_2$  compounds with new surfaces.

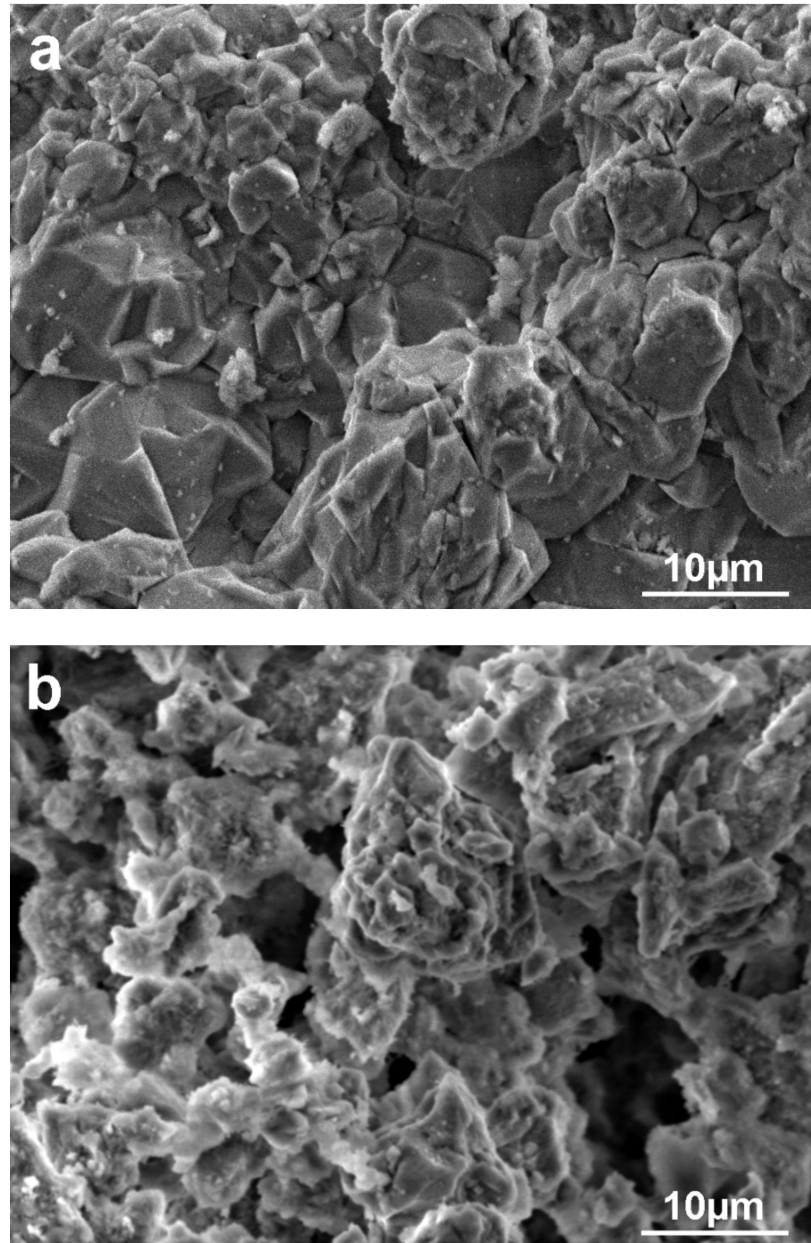
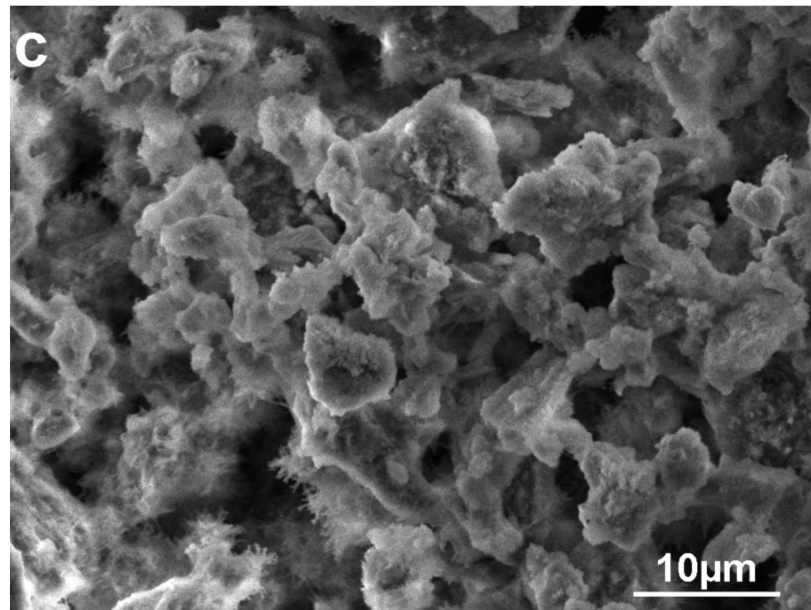
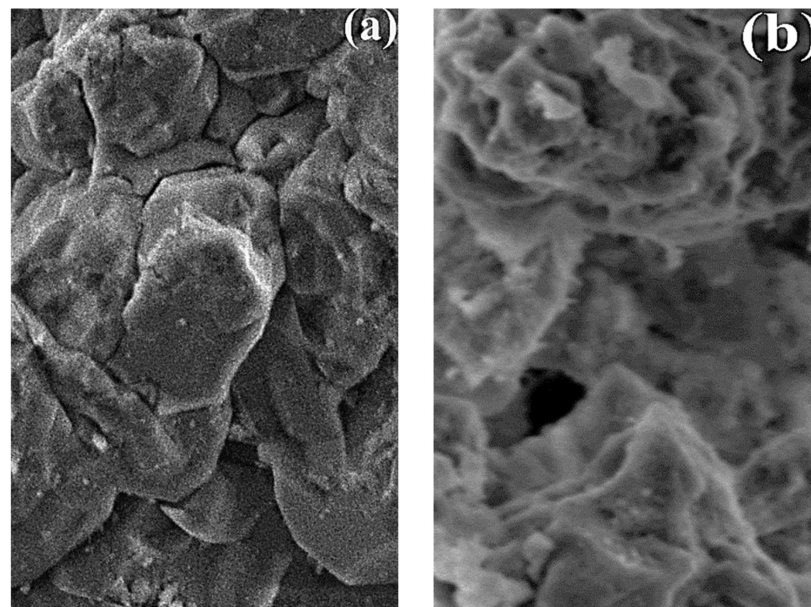


Figure 2. Cont.



**Figure 2.** Variable pressure scanning electron microscopy images of SiO<sub>2</sub>: (a) SiO<sub>2</sub> SilB sample, (b) SiO<sub>2</sub> Siland sample without dispersion, and (c) SiO<sub>2</sub> Silad3.5 sample with dispersion.

Some details of each image are presented in Figure 3. Clearly, the surface state of the grains for the non-dispersed and dispersed samples compared to the starting sample is evidenced. It is very important to point out the change in the grain surface state, which would have an important role in determining the properties of composite-charge interfaces.



**Figure 3.** *Cont.*

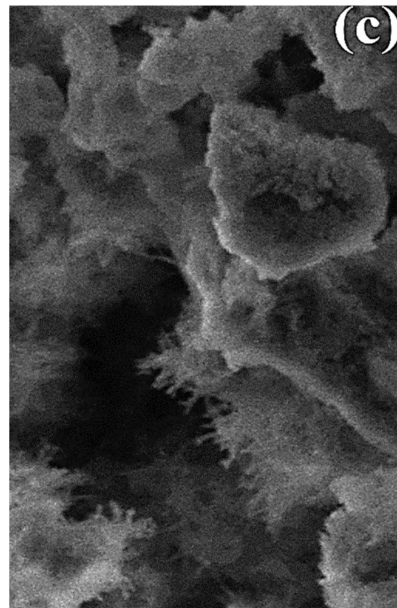


**Figure 3.** An insert from VP-SEM images of Figure 2, (a) SiO<sub>2</sub> SilB sample, (b) SiO<sub>2</sub> Siland sample without dispersion, and (c) SiO<sub>2</sub> Silad3.5 sample with dispersion.

Figure 4 shows the EDS analysis of the zones of the images depicted in Figure 2. The peaks corresponding to the silicon and oxygen elements of the SiO<sub>2</sub> compound are clearly seen. The observed carbon content is attributed to the sample holder. In fact, this analysis shows the successful treatment process developed in this study.

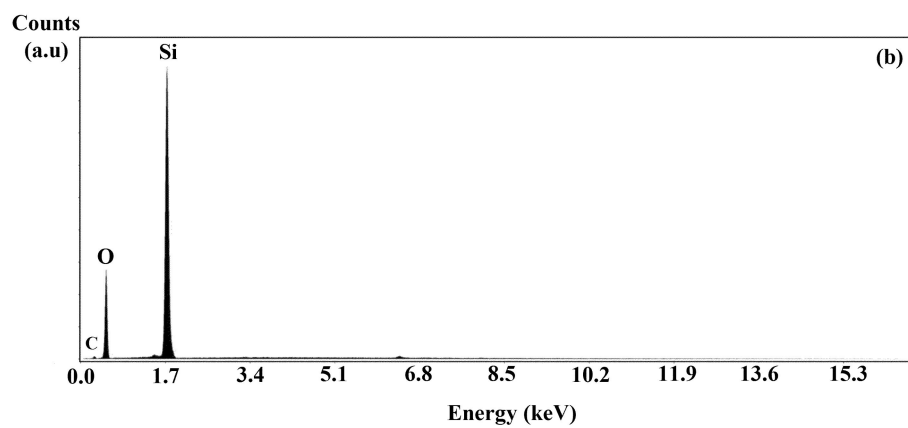
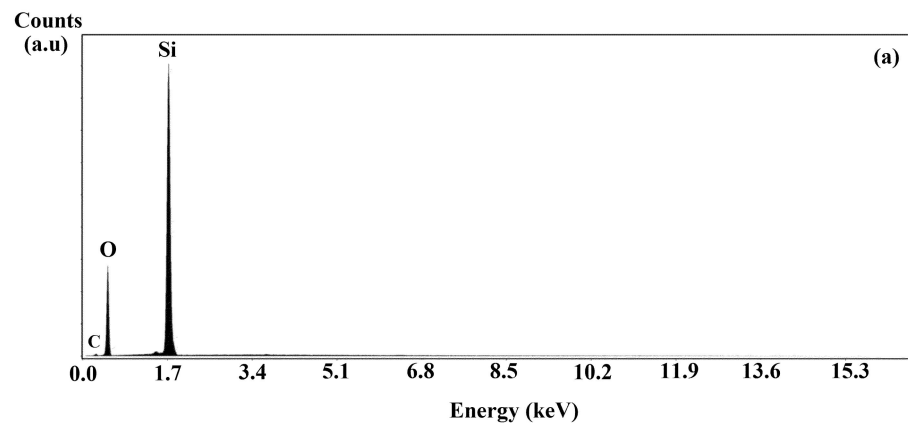


**Figure 4.** *Cont.*

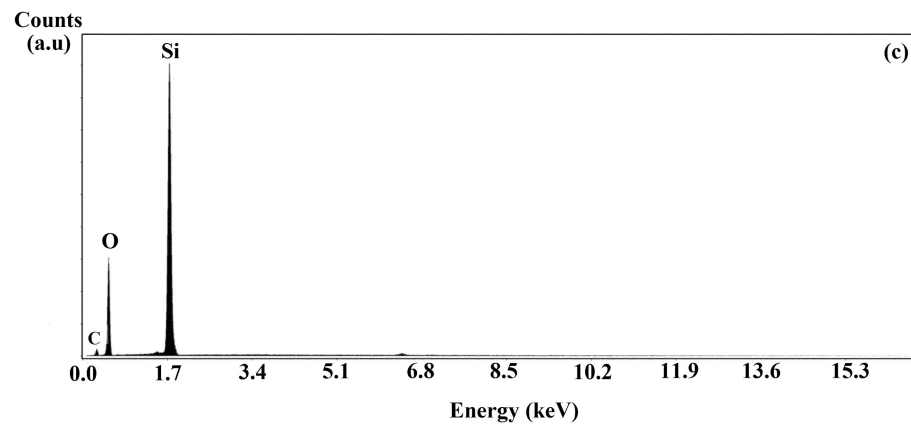


**Figure 4.** EDS spectra corresponding to the zones of the images in Figure 2, (a) SiO<sub>2</sub> SilB sample, (b) SiO<sub>2</sub> Siland sample without dispersion, and (c) SiO<sub>2</sub> Silad3.5 sample with dispersion.

### 3.2. High-Resolution Transmission Electron Microscopy (HR-TEM)

High-resolution transmission electron microscopy (HR-TEM) and energy-dispersive X-ray spectroscopy (EDS) are employed to investigate the morphology, nanostructures, and composition of 1D nano-fibrous SiO<sub>2</sub> surface. As presented in Figure 3c for dispersed SiO<sub>2</sub> sample, the surface of the grains appears the silica nanofibers. For more insights into the silica fibers' behaviors, the sample is observed through HR-TEM. The HR-TEM images (Figure 5a,b) indicate various morphologies of nanofibers silica were taken place on the SiO<sub>2</sub> surface. After deposition, nano-SiO<sub>2</sub> fibers with a length of 20–250 nm were formed on the surface.

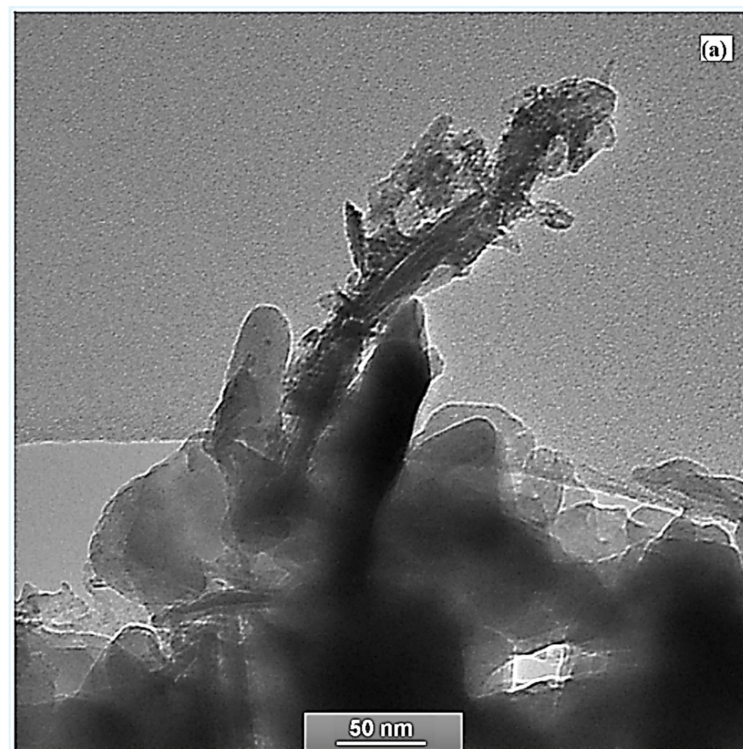


**Figure 5.** Cont.

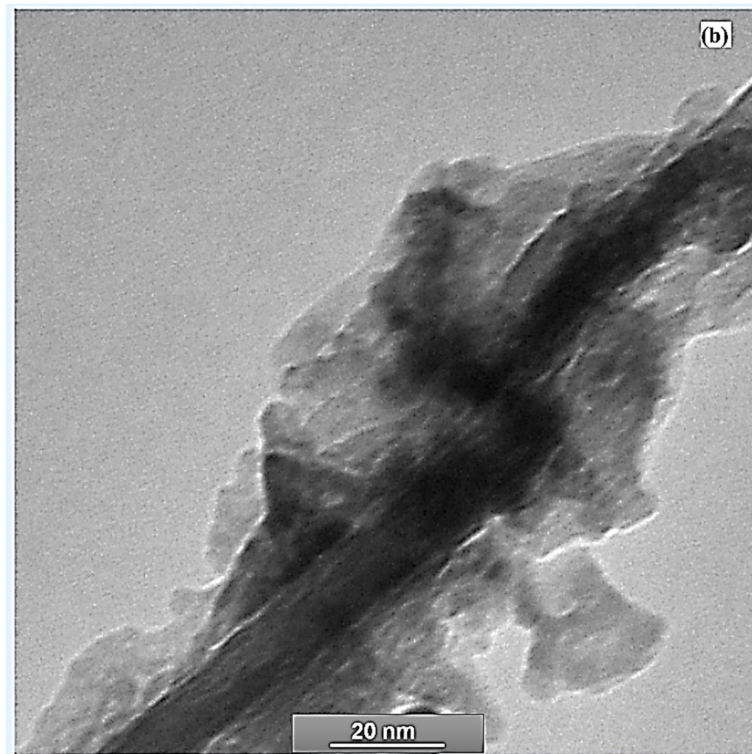


**Figure 5.** HR-TEM images for silica nanofibers on the surface of SiO<sub>2</sub> with dispersion (Silad3.5): (a) 50 nm scale (b) 20 nm scale.

This observation provides favorable evidence for the presence of nano-fibrous SiO<sub>2</sub> surface, supporting the VP-SEM observation in Figures 2c and 3c. It appeared that the nano-SiO<sub>2</sub> fibers adhered to the surface cohesively, which proved the strong surfacial bonding between the nano SiO<sub>2</sub> fiber and the SiO<sub>2</sub> network. The analysis of the nanofibers shows the pure SiO<sub>2</sub> basic unit.

### 3.3. Fourier Transformed Infrared Spectroscopy (FTIR) and X-ray Photoelectron Spectroscopy XPS

In Infrared spectroscopy, interatomic bonds (Si-O-Si and Si-O-H as examples) absorb infrared light of its resonant. The evolution of the interatomic bonds vibrations is followed by recording IR spectra of the different samples. The FTIR spectra between 400 cm<sup>-1</sup> and 1400 cm<sup>-1</sup> of the samples SilB, Siland, and Silad3.5 are presented in Figure 6. The infrared spectrum of all samples has a broadband between 1000 and 1300 cm<sup>-1</sup>. This band consists of two strong peaks located at 1078 cm<sup>-1</sup> and 1163 cm<sup>-1</sup>. These peaks are associated with the stretching vibration of Si-O-Si [24–28]. In addition, bending vibrations attributed to Si-O-Si [26–28] located at 455, 509, 778, and 800 cm<sup>-1</sup> are observed in the spectrum. The bands located at 555 cm<sup>-1</sup> and 950 cm<sup>-1</sup> are associated with Si-O bending vibrations of non-bridging Si-OH bonds and stretching vibration respectively [29–31].

Non-bridging Si-O bonds are formed when H<sup>+</sup> occupies the residual charge of non-bridging Si-O<sup>-</sup>, forming Si-OH. Thus, the resulting Si-O vibration is expected to have a higher natural frequency than Si-O vibrations in bridging Si-O-Si. In fact,  $\nu$ Si-O in Si-OH is not directly influenced by another Si of the crystal lattice in its vicinity, as is the case for  $\nu$ Si-O in Si-O-Si. Bonding of Si-O with another Si of the lattice lowers  $\nu$ Si-O when compared to the free vibration in Si-OH. This kind of non-bridging Si-O bending vibration can also be expected in hydroxylated silica glass-like opal-A where a part of the Si-O-Si bonds are interrupted by the incorporation of hydrogen protons [32].

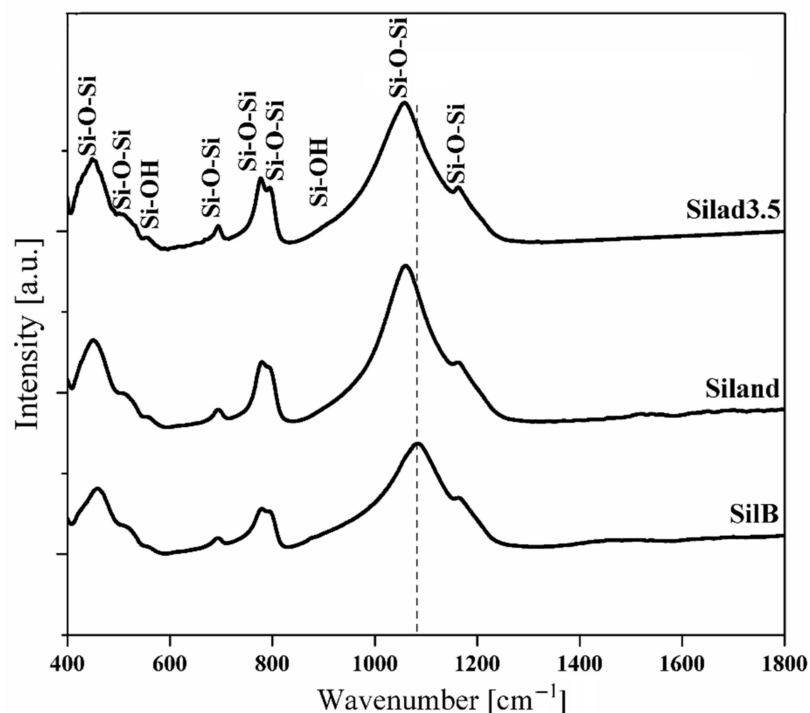


Figure 6. FTIR spectra of samples SilB, Siland, and Silad3.5.

Figure 6 shows that the mean band of samples spectra after the reaction is shifted compared to SilB before the reaction as reference. A pronounced shift of the main band towards the low wavenumber is observed and can be attributed to the structural order change of  $\text{SiO}_2$  and the surface state of the samples compared to SilB reference. The evolution of the intensity ratio between Si-OH band located around  $555 \text{ cm}^{-1}$  and the structural band located around  $500 \text{ cm}^{-1}$  is related to the vibration Si-O-Si as shown in Figure 7.

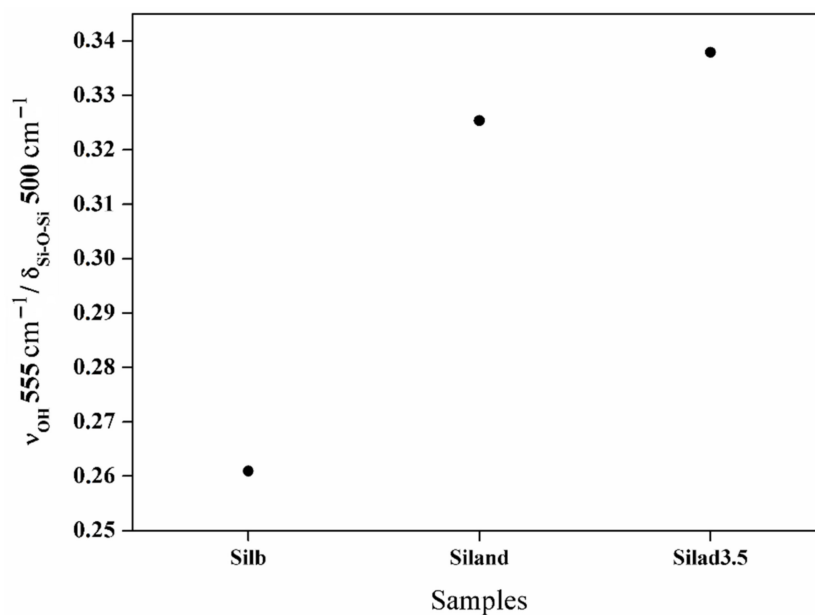


Figure 7. The evolution of the intensity ratio between Si-OH band located around  $555 \text{ cm}^{-1}$  and the structural band located around  $500 \text{ cm}^{-1}$ .

The intensity ratio between Si-OH band and Si-O-Si increases with the reaction. This evolution proves the formation of Si-OH bonds and the change of the SiO<sub>2</sub> surface is in agreement with the results observed by VP-SEM. These results corroborate the surface silica change obtained with SEM characterization.

XPS is a highly sensitive technique used to examine the composition and chemical states of a surface. In fact, important changes in the chemical bonding environments result in important shifts in the photoelectron energy, thus allowing chemical information to be obtained. Different chemical properties may be obtained from the binding energies such as oxidation state, nearest neighbor atoms, and type of bonding [33].

Additionally, the surface of silicon substrates treated with NaOH using XPS have investigated [34]. The shift of O1s photoelectron peaks is attributed to the amount of Si-OH, which increases with the treatment [35]. In addition, the reported experimental work indicated that XPS analysis may be used to obtain detailed information on the hydrolysis and condensation reactions occurring during the synthesis of the inorganic materials. Figure 8 shows the O1s XPS and Si2p spectra of the sample before and after treatment. The binding energy shifting of the Si2p and O1s photoelectron peaks have been observed (Figure 8a,b).

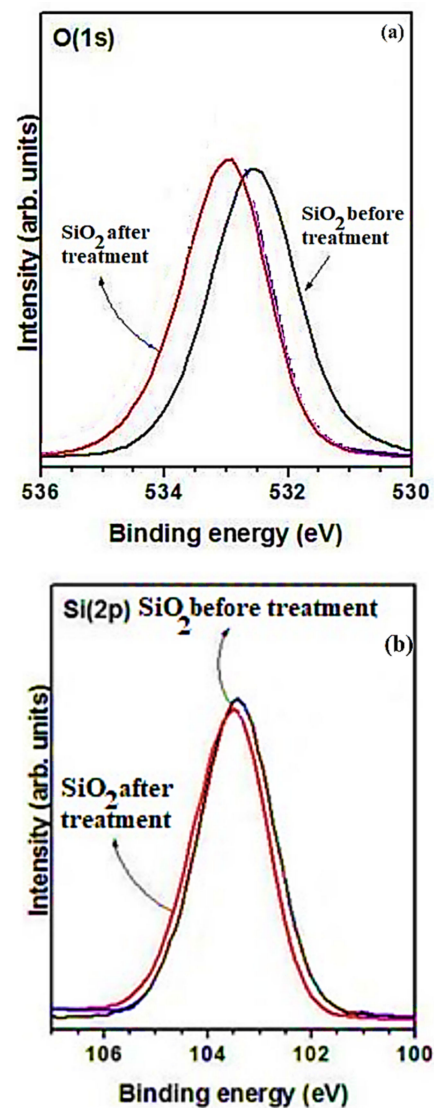
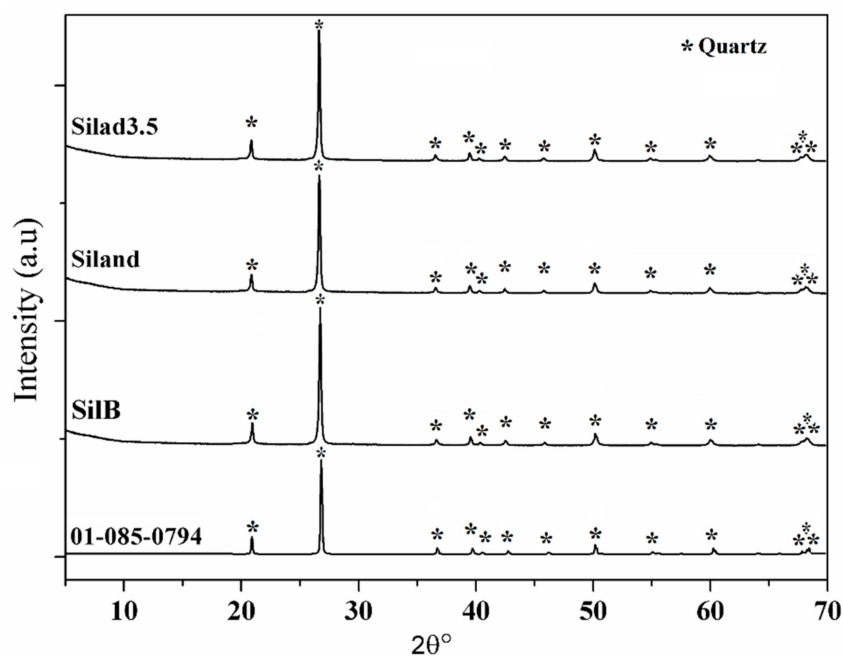


Figure 8. XPS spectra of SiO<sub>2</sub> before and after treatment (a) O1s, (b) Si2p.

The results showed variation in silicon and oxygen threshold changes. In addition, the O1s photoelectron peak tends to shift to higher binding energies which may be ascribed to an increase in the number of silanol groups [34]. The shift is very important showing that the environment of oxygen on the surface is affected which is in agreement with the FTIR results.

### 3.4. X-ray Diffraction Results

Figure 9 shows XRD patterns of the aggregate before the reaction (SilB) used as reference. In the aggregate, the pattern is identified as hexagonal related to the SiO<sub>2</sub> crystalline phase corresponding to the file [PDF 01-085-0794]. XRD patterns of the samples Silad and Silad3.5 after the reaction compared to reference SilB are presented as well. Peaks referred to as quartz phase crystals are present in all samples proving that whatever the treatment, the SiO<sub>2</sub> lattice is maintained and the protocol developed allows the conservation of the initial structure of SiO<sub>2</sub>.



**Figure 9.** XRD patterns of SilB, Silad, and Silad3.5 samples.

In order to follow intrinsic changes, the highest peak diffraction (101) for the three samples is compared as shown in Figure 10. It can be clearly seen after the treatment, a shift of this peak towards the small angles with respect to the compound before treatment SilB. These results are in good agreement with those obtained with FTIR and confirmed with the increase of silanols content in the surface. In addition, this shift can also be explained by an expansion effect of the SiO<sub>2</sub> structure after treatment as indicated in Figure 10.

The schematically interpretation of multistep formation simplified mechanism of 1D nano-fibrous SiO<sub>2</sub> surfaces with controlled SiOH silanol amount is given in Figure 11a,b. At first, it can be seen that the starting 3D SiO<sub>2</sub> framework is preserved. After dispersion, the formation of the nano-fibrous SiO<sub>2</sub> surfaces on the one hand, then the formation of SiOH silanols is observed (Figure 11b).

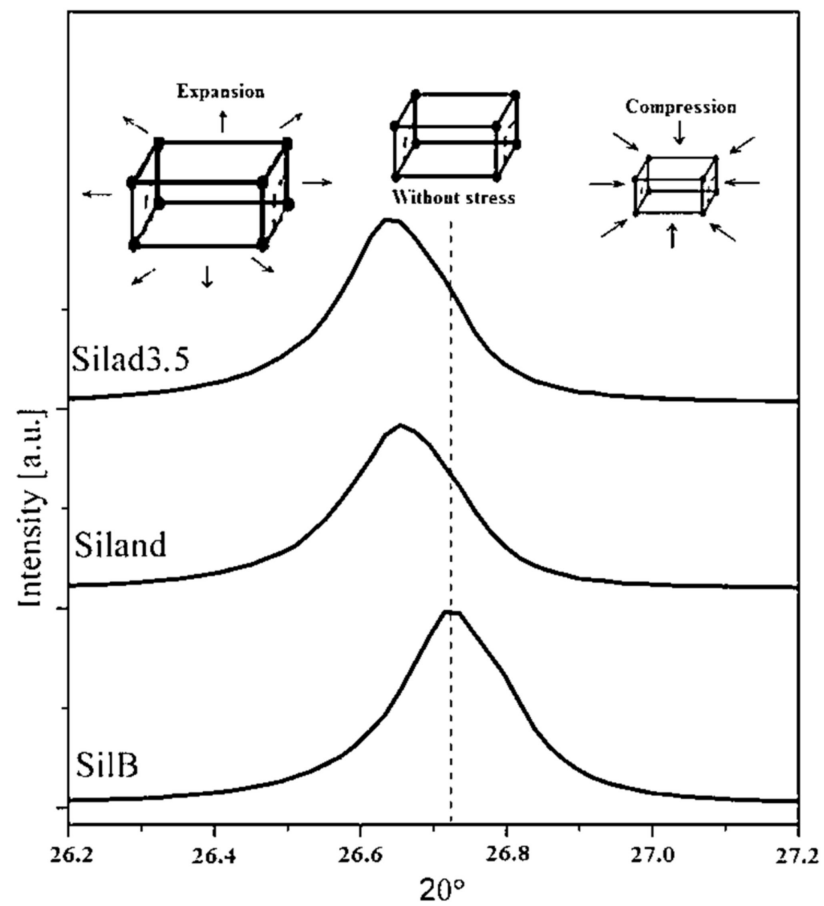


Figure 10. XRD (101) main peak of SilB, Siland, and Silad3.5 samples.

The presence of silanols and of nano-fibrous surface presents a double advantage for the improvement of the interaction at the interfaces between  $\text{SiO}_2$  and certain organic surfaces such as polymers and/or asphalt for example.

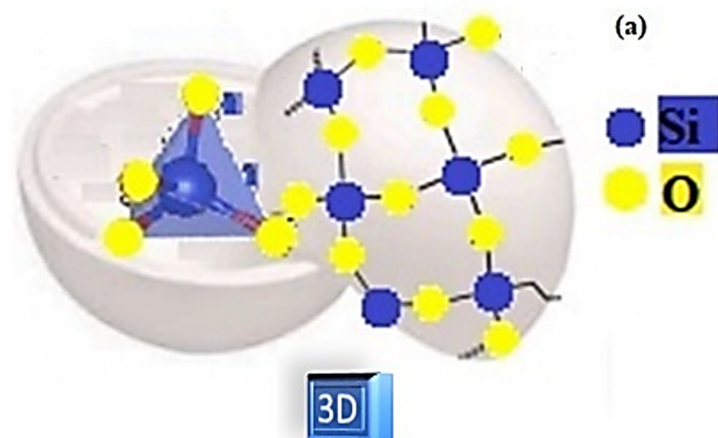
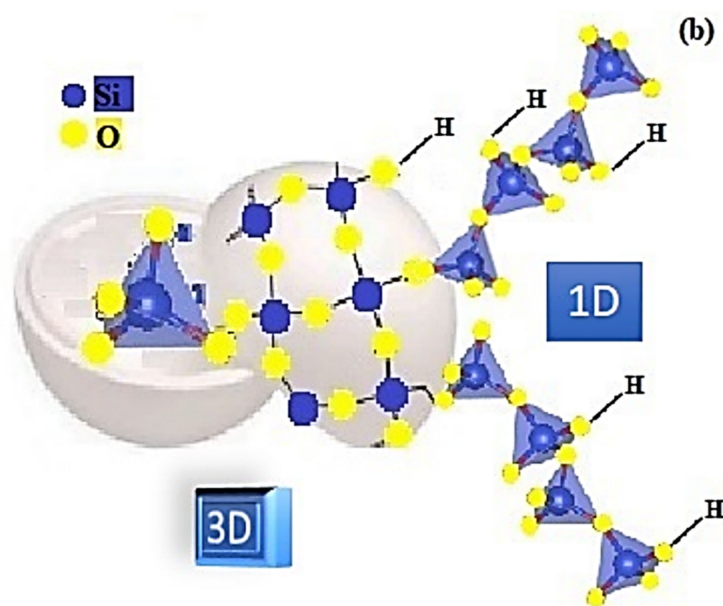


Figure 11. Cont.



**Figure 11.** The proposed simplified schematic illustrations showing the surface functionalization of  $\text{SiO}_2$ , (a) before treatment, (b) after treatment.

#### 4. Conclusions

In the present article, natural  $\text{SiO}_2$  surfaces with nanofibers are obtained, and the effect of HCl dispersion on the functionalization process is well demonstrated. Morphological and chemical properties of obtained samples were investigated by VP-SEM, EDS, HR-TEM, FTIR, XPS spectroscopy, and XRD techniques. The fabricated  $\text{SiO}_2$  samples exhibited a high pure and original surface. Our results indicate the presence of nanofibers and prove the presence of SiOH groups on the  $\text{SiO}_2$  surface as confirmed by HR-TEM.

A surface functionalization protocol under optimal conditions is developed. The results of this study show that the effectiveness of the protocol is multiple:

1. it allows the chemical functionalization of the surface with controlled SiOH silanols amount,
2. it allows the fabrication of nano-fibrous surfaces, observed and confirmed by several microscopy methods as corroborated by HR-TEM showing the presence of  $\text{SiO}_2$  nanofibers on the surface of lengths ranging from 20 nm to 250 nm,
3. it keeps the structural state of the starting 3D  $\text{SiO}_2$  framework,
4. The method developed is free of any polluting compounds,
5. The method developed is 100% mineral and free of any organic compound.

The compounds obtained with original surfaces and a simple and less expensive method are in use in order to overcome the poor interfacial bonding strength between  $\text{SiO}_2$  compounds and polymer (or organic materials).

**Author Contributions:** Conceptualization, L.K.; methodology, L.K. and A.O.; software, L.K. and A.O.; validation, L.K. and A.O.; formal analysis, A.O.; investigation, L.K. and A.O.; resources, L.K.; data curation, L.K. and A.O.; writing—original draft preparation, L.K.; writing—review and editing, L.K. and A.O.; visualization, L.K. and A.O.; supervision, L.K. and A.O.; project administration, L.K.; funding acquisition, L.K. and A.O. All authors have read and agreed to the published version of the manuscript.

**Funding:** Part of this research was funded FEDER, Institut Chevreul USTL-France, and Analysis and Characterization Center (CAC)-Morocco.

**Acknowledgments:** Part of this research was funded European Community funding FEDER, Institut Chevreul USTL-France, and Analysis and Characterization Center (CAC)-Morocco. The authors thank M. Elaatmani and Zegzouti for the discussion.

**Conflicts of Interest:** The authors declare no conflict of interest.

## References

1. Sarikaya, E.; Çallioğlu, H.; Demirel, H. Production of epoxy composites reinforced by different natural fibers and their mechanical properties. *Compos. Part B Eng.* **2019**, *167*, 461–466. [[CrossRef](#)]
2. Oertel, T.; Hutter, F.; Helbig, U.; SEXTL, G. Amorphous silica in ultra-high performance concrete: First hour of hydration. *Cem. Concr. Res.* **2014**, *58*, 131–142. [[CrossRef](#)]
3. Khouchaf, L.; Boulahya, K.; Das, P.P.; Nicolopoulos, S.; Kis, V.K.; Lábár, J.L. Microstructure study of Amorphous Silica nanostructure using High Resolution Electron Microscopy, Electron Energy Loss Spectroscopy, X-ray Powder Diffraction and Electron Pair Distribution Function. *Materials* **2020**, *13*, 4393. [[CrossRef](#)] [[PubMed](#)]
4. Khouchaf, L.; Boinski, F.; Tuilier, M.; Flank, A. Characterization of heterogeneous SiO<sub>2</sub> materials by scanning electron microscope and micro fluorescence XAS techniques. *Nucl. Instrum. Methods Phys. Res. Sect. B Beam Interact. Mater. At.* **2006**, *252*, 333–338. [[CrossRef](#)]
5. Price, P.M.; Clark, J.H.; Macquarrie, D.J. Modified silicas for clean technology. *J. Chem. Soc. Dalton Trans.* **2000**, *52*, 101–110. [[CrossRef](#)]
6. Cauqui, M.; Rodríguez-Izquierdo, J.M. Application of the sol-gel methods to catalyst preparation. *J. Non-Cryst. Solids* **1992**, *147–148*, 724–738. [[CrossRef](#)]
7. Nicollian, E.H.; Brews, J.R. *Metal Oxide Semiconductor. Physics and Technology*; WILEY-VCK: New York, NY, USA, 2002.
8. Muthalvan, R.S.; Ravikumar, S.; Avudaiappan, S.; Amran, M.; Aepuru, R.; Vatin, N.; Fediuk, R. The Effect of Superabsorbent Polymer and Nano-Silica on the Properties of Blended Cement. *Crystals* **2021**, *11*, 1394. [[CrossRef](#)]
9. Zou, H.; Wu, S.; Shen, J. Polymer/Silica Nanocomposites: Preparation, Characterization, Properties, and Applications. *Chem. Rev.* **2008**, *108*, 3893–3957. [[CrossRef](#)]
10. Song, X.; Xu, H.; Zhou, D.; Yao, K.; Tao, F.; Jiang, P.; Wang, W. Mechanical Performance and Microscopic Mechanism of Coastal Cemented Soil Modified by Iron Tailings and Nano Silica. *Crystals* **2021**, *11*, 1331. [[CrossRef](#)]
11. Ren, Z.; Zhou, W.; Qing, Y.; Duan, S.; Pan, H.; Zhou, Y. Improved mechanical and microwave absorption properties of SiCf/SiC composites with SiO<sub>2</sub> filler. *Ceram. Int.* **2021**, *47*, 14455–14463. [[CrossRef](#)]
12. Tahiri, N.; Khouchaf, L.; Elaamrani, M.; Louarn, G.; Zegzouti, A.; Daoud, M. Study of the thermal treatment of SiO<sub>2</sub> aggregate. *IOP Conf. Ser. Mater. Sci. Eng.* **2014**, *62*, 012002. [[CrossRef](#)]
13. Tran, H.-B.; Le, V.-B.; Phan, V.T.-A. Mechanical Properties of High Strength Concrete Containing Nano SiO<sub>2</sub> Made from Rice Husk Ash in Southern Vietnam. *Crystals* **2021**, *11*, 932. [[CrossRef](#)]
14. Zhang, Q.; Pang, X.; Zhao, Y. Effect of the External Velocity on the Exfoliation Properties of Graphene from Amorphous SiO<sub>2</sub> Surface. *Crystals* **2021**, *11*, 454. [[CrossRef](#)]
15. Yang, L.; Wang, X.; Qiu, Q.; Gao, J.; Tang, C. The effect of surface hydroxylation of Nano-SiO<sub>2</sub> on the insulating paper cellulose/Nano-SiO<sub>2</sub> interface. *Mater. Chem. Phys.* **2021**, *260*, 124124. [[CrossRef](#)]
16. Boinski, F.; Khouchaf, L.; Tuilier, M.-H. Study of the mechanisms involved in reactive silica. *Mater. Chem. Phys.* **2010**, *122*, 311–315. [[CrossRef](#)]
17. Tian, S.; Gao, W.; Liu, Y.; Kang, W.; Yang, H. Effects of surface modification Nano-SiO<sub>2</sub> and its combination with surfactant on interfacial tension and emulsion stability. *Colloids Surf. A* **2020**, *595*, 124682. [[CrossRef](#)]
18. Hunter, R.J. *Zeta Potentiel in Colloid Science*; Academic Press Inc.: San Diego, CA, USA, 1988.
19. Iler, R.K. *The Chemistry of Silica*; Wiley-Interscience: New York, NY, USA, 1979.
20. Sassi, W.; Dhoubi, L.; Berçot, P.; Rezrazi, M. The effect of SiO<sub>2</sub> nanoparticles dispersion on physico-chemical properties of modified Ni–W nanocomposite coatings. *Appl. Surf. Sci.* **2015**, *324*, 369–379. [[CrossRef](#)]
21. Fidalgo, A.; Rosa, M.E.; Ilharco, L.M. Chemical Control of Highly Porous Silica Xerogels: Physical Properties and Morphology. *Chem. Mater.* **2003**, *15*, 2186–2192. [[CrossRef](#)]
22. Huang, Q.; Gu, M.; Sun, K.; Jin, Y. Effect of pretreatment on rheological properties of silicon carbide aqueous suspension. *Ceram. Int.* **2002**, *28*, 747–754. [[CrossRef](#)]
23. Shin, Y.; Lee, D.; Lee, K.; Ahn, K.H.; Kim, B. Surface properties of silica nanoparticles modified with polymers for polymer nanocomposite applications. *J. Ind. Eng. Chem.* **2008**, *14*, 515–519. [[CrossRef](#)]
24. Korovkin, M.V.; Ananieva, L.G.; Antsiferova, A.A. Assessment of quartzite crystallinity index by FT-IR. In Proceedings of the 10th International Congress for Applied Mineralogy (ICAM), Trondheim, Heidelberg, 20 March 2012.
25. Barbosa, G.N.; Oliveira, H.P. Synthesis and characterization of V<sub>2</sub>O<sub>5</sub>–SiO<sub>2</sub> xerogel composites prepared by base catalysed sol–gel method. *J. Non-Cryst. Solids* **2006**, *352*, 3009–3014. [[CrossRef](#)]
26. Kim, H.-U.; Rhee, S.-W. Electrical Properties of Bulk Silicon Dioxide and SiO<sub>2</sub>/Si Interface Formed by Tetraethylorthosilicate Ozone Chemical Vapor Deposition. *J. Electrochem. Soc.* **2000**, *147*, 1473. [[CrossRef](#)]
27. Chen, Z.-L.; Shen, P. Thermally activated sintering–coarsening–coalescence–polymerization of amorphous silica nanoparticles. *Ceram. Int.* **2013**, *39*, 2365–2373. [[CrossRef](#)]
28. Jung, K.T.; Chu, Y.-H.; Haam, S.; Shul, Y.G. Synthesis of mesoporous silica fiber using spinning method. *J. Non-Crystalline Solids* **2002**, *298*, 193–201. [[CrossRef](#)]

29. Schmidt, P.; Fröhlich, F. Temperature dependent crystallographic transformations in chalcedony, SiO<sub>2</sub>, assessed in mid infrared spectroscopy. *Spectrochim. Acta Part A Mol. Biomol. Spectrosc.* **2011**, *78*, 1476–1481. [[CrossRef](#)]
30. Schmidt, P.; Badou, A.; Fröhlich, F. Detailed FT near-infrared study of the behaviour of water and hydroxyl in sedimentary length-fast chalcedony, SiO<sub>2</sub>, upon heat treatment. *Spectrochim. Acta Part A Mol. Biomol. Spectrosc.* **2011**, *81*, 552–559. [[CrossRef](#)]
31. Domanski, M.; Webb, J. Effect of heat treatment on siliceous rocks used in prehistoric lithic technology. *J. Archaeol. Sci.* **1992**, *19*, 601–614. [[CrossRef](#)]
32. Langer, K.; Flörke, O.W. Near Infrared Absorption Spectra (4000–9000 cm<sup>-1</sup>) of Opals and the Role of “Water” in These SiO<sub>2</sub>.nH<sub>2</sub>O Minerals. *Fortschr. Mineral.* **1974**, *53*, 17–51.
33. Black, L.; Garbev, K.; Stemmermann, P.; Hallam, K.R.; Allen, G.C. Characterisation of crystalline C-S-H phases by X-ray photoelectron spectroscopy. *Cem. Concr. Res.* **2003**, *33*, 899–911. [[CrossRef](#)]
34. Miyaji, F.; Iwai, M.; Kokubo, T.; Nakamura, T. Chemical surface treatment of silicone for inducing its bioactivity. *J. Mater. Sci. Mater. Med.* **1998**, *9*, 61–65. [[CrossRef](#)]
35. Oufakir, A.; Khouchaf, L.; Elaammani, M.; Zegzouti, A.; Louarn, G.; Ben Fraj, A. Study of structural short order and surface changes of SiO<sub>2</sub> compounds. *MATEC Web Conf.* **2018**, *149*, 01041. [[CrossRef](#)]